LBL-37814
UC-411

Lawrence Berkeley Laboratory

UNIVERSITY OF CALIFORNIA

CHEMICAL SCIENCES DIVISION

To be presented at the XXth International Solvay Conference in Chemistry, Brussels, Belgium, November 28–December 2, 1995, and to be published in Quantum and Semiclassical Theories of Chemical Reaction Rates

Quantum and Semiclassical Theories of Chemical Reaction Rates

W.H. Miller

September 1995

REFERENCE COPY
Does Not
Circulate
Bldg. 50 Library.
LBL-37814
Copy 1

Prepared for the U.S. Department of Energy under Contract Number DE-AC03-76SF00098

DISCLAIMER

This document was prepared as an account of work sponsored by the United States Government. While this document is believed to contain correct information, neither the United States Government nor any agency thereof, nor the Regents of the University of California, nor any of their employees, makes any warranty, express or implied, or assumes any legal responsibility for the accuracy, completeness, or usefulness of any information, apparatus, product, or process disclosed, or represents that its use would not infringe privately owned rights. Reference herein to any specific commercial product, process, or service by its trade name, trademark, manufacturer, or otherwise, does not necessarily constitute or imply its endorsement, recommendation, or favoring by the United States Government or any agency thereof, or the Regents of the University of California. The views and opinions of authors expressed herein do not necessarily state or reflect those of the United States Government or any agency thereof or the Regents of the University of California.

LBL-37814
UC-411

Quantum and Semiclassical Theories of Chemical Reaction Rates

William H. Miller

Department of Chemistry
University of California, Berkeley

and

Chemical Sciences Division
Lawrence Berkeley National Laboratory
University of California
Berkeley, California 94720

September 1995

This work was supported by the Director, Office of Energy Research, Office of Basic Energy Sciences, Chemical Sciences Division, of the U.S. Department of Energy under Contract No. DE-AC03-76SF00098.

LBL#-37814

Quantum and Semiclassical Theories of Chemical Reaction Rates

William H. Miller

Department of Chemistry, University of California, and

Chemical Sciences Division, Lawrence Berkeley National Laboratory,

Berkeley, California 94720

Abstract

A rigorous quantum mechanical theory (and a semiclassical approximation thereto) is described for calculating chemical reaction rates "directly", i.e., without having to solve the complete state-to- state reactive scattering problem. The approach has many vestiges of transition state theory, for which it may be thought of as the rigorous generalization.

I. INTRODUCTION

The rate constant for a chemical reaction is conveniently expressed in terms of the *cumulative reaction probability*[1] (CRP) N(E),

$$N(E) \equiv \sum_{\mathbf{n}_r,\mathbf{n}_p} |S_{\mathbf{n}_p,\mathbf{n}_r}(E)|^2, \tag{1.1}$$

where the S-matrix elements must in general be determined by solving the state-to-state reactive scattering Schrödinger equation. ($\mathbf{n}_r$ and $\mathbf{n}_p$ denote the asymptotic quantum states of reactants and products.) The microcanonical rate constant for total energy E, typically the quantity of interest for unimolecular reactions, is given in terms of the CRP by

$$k(E) = [2\pi\hbar\rho_r(E)]^{-1}N(E), \tag{1.2}$$

where ρ_r is the density of reactant states per unit energy, and the canonical (or thermal) rate constant is the Boltzmann average of the CRP,

$$k(T) = [2\pi\hbar Q_r(T)]^{-1}\int_{-\infty}^{\infty} dE\; e^{-E/kT}N(E), \tag{1.3}$$

where Q_r is the reactant partition function per unit volume.

Considerable progress has been made in recent years[2–4] in learning how to calculate the CRP more *directly* than via Eq. (1.1), i.e., without having to solve explicitly for the S-matrix, yet still *correctly*, i.e., without any inherent approximations. It is still necessary to determine the quantum dynamics of the system, but typically only for short times and only in the interaction region where the reactive flux is determined, not in the longer range regions that determine the distributions of reactant and product quantum states. The overall approach has very much the "feel" of transition state theory,[5,6] though it is a fully rigorous ("exact") quantum treatment. Section II briefly reviews this rigorous quantum approach for obtaining the CRP and its various applications to date.

Even with the progress that has been made in rigorous quantum approaches it is nevertheless possible to carry out such calculations only for relatively simple chemical systems. E.g., the largest molecular system for which such calculations have been carried out is for

the reaction $H_2 + OH \rightarrow H_2O + H$. There is clearly interest, therefore, in the development of approximate versions of the approach that can be applied to more complex systems. Section III describes a semiclassical approximation for doing this, and Section IV concludes.

II. QUANTUM THEORY

Miller, Schwartz, and Tromp[2] showed more than ten years ago that the CRP can be expressed exactly in terms of the microcanonical density operator,

$$N(E) = \frac{1}{2}(2\pi\hbar)^2 \, tr\,[\hat{F}\delta(E-\hat{H})\,\hat{F}\,\delta(E-\hat{H})\,], \tag{2.1}$$

where $\hat{H}$ is the Hamiltonian operator of the molecular system and $\hat{F}$ is a flux operator defined with respect to a dividing surface which separates reactants and products. (The value of N(E) is independent of the location of the dividing surface.) The task is then to find an efficient way to compute matrix elements of the density operator $\delta(E-\hat{H})$.

Thirumalai *et al.*[7] noted that one can use a Gaussian pre-limit representation of the delta function,

$$\begin{aligned}\delta(E-\hat{H}) &= \left(\frac{\alpha}{\pi}\right)^{\frac{1}{2}} e^{-\alpha(\hat{H}-E)^2} \\ &= \left(\frac{M\Delta\alpha}{\pi}\right)^{\frac{1}{2}} \left[e^{-\Delta\alpha(\hat{H}-E)^2}\right]^M,\end{aligned} \tag{2.2}$$

to do the job. If $\Delta\alpha \equiv \alpha/M$ is sufficiently small, then a "short time"-like approximation can be used to obtain the matrix representation of exp[-$\Delta\alpha(\hat{H}-E)^2$], and then the full result in Eq. (2.2) is obtained by matrix multiplication. This approach was seen to work well in some simple examples.

A more powerful approach was presented by Seideman *et al.*,[3]

$$\delta(E-\hat{H}) = -\frac{1}{\pi} Im\hat{G}(E), \tag{2.3a}$$

with

$$\hat{G}(E) = (E + i\hat{\epsilon} - \hat{H})^{-1}, \tag{2.3b}$$

where $\hat{\epsilon}$ is an absorbing potential[8] energy operator. If $\hat{\epsilon}$ were chosen to be a constant, as in the conventional definition of the Green's function, then Eq. (2.3) is a Lorentzian pre-limit representation of the delta function,

$$\Delta(E\hat{H}) \cong \frac{\epsilon}{\pi}[(\hat{H}-E)^2+\epsilon^2]^{-1}, \tag{2.4}$$

but the power of Eq. (2.3) is that $\hat{\epsilon}$ need not be a constant. By allowing it to be a potential energy operator one can choose it to be essentially zero in the interaction region, where the relevant reaction dynamics takes place, and "turn it on" gradually in the reactant and product exit valleys; this in effect imposes outgoing wave boundary conditions for a L^2 representation of the Green's function in Eq. (2.3b). Figure 1 shows a contour plot of the potential energy surface for the $H+H_2 \rightarrow H_2+H$ reaction and the absorbing potential. (The points in Fig. 1 are the grid points for a discrete variable representation of the Hamiltonian operator.)

From a time-dependent point of view, the absorbing potential damps the time-dependent wave packet as it exits the interaction region and thus prevents reflection from the edge of the grid, thereby enforcing the outgoing wave boundary condition. In practice one wishes to "turn on" the absorbing potential as rapidly as possible - so as to keep the grid (i.e., basis set) as small as possible - but not so rapidly as to cause unphysical reflections.

With the microcanonical density operator given by Eq. (2.3), Seideman *et al.*[3] then showed that Eq. (2.1) for the CRP takes the simpler form

$$N(E) = 4tr[\hat{G}(E)^*\hat{\epsilon}_p\hat{G}(E)\hat{\epsilon}_r], \tag{2.5}$$

with the Green's function given by Eq. (2.3b) and where $\hat{\epsilon}_r(\hat{\epsilon}_p)$ is the part of the absorbing potential in the reactant (product) exit valley. Note that in Eq. (2.5) there is no longer any reference to a "dividing surface", now only a "dividing region", the space between the two absorbing potentials. Eq. (2.5) corresponds effectively to solving the Schrödinger equation (equivalent to constructing the Green's function) through this interaction region, revealing again the qualitative "transition state" nature of the formulation.

Finally, Manthe *et al.*[4] have shown that for large systems Eq. (2.5) can be evaluated most efficiently by writing it as

$$N(E) = tr\,[\hat{P}(E)], \tag{2.6a}$$

where

$$\hat{P}(E) = 4\hat{\epsilon}_r^{1/2}\hat{G}(E)^*\hat{\epsilon}_p\hat{G}(E)\hat{\epsilon}_r^{1/2}. \tag{2.6b}$$

The *reaction probability operator* $\hat{P}$ of Eq. (2.6b) is hermitian, and clearly positive, and one can furthermore show[4] that it is bounded by the identity operator, i.e.,

$$0 < \hat{P}(E) < 1. \tag{2.7}$$

The eigenvalues of $\hat{P}$, $\{p_k(E)\}$, thus lie between 0 and 1 and can therefore be interpreted as probabilities, the *eigen reaction probabilities*, the sum of which gives the CRP,

$$N(E) = \sum_k p_k(E). \tag{2.8}$$

The reason that Eqs. (2.6)-(2.8) are so efficient computationally is that the rank of $\hat{P}$(E), i.e., the number of its eigenvalues that are significantly different from zero, is in general quite low compared to the dimension of the matrix itself (which is the dimension of the Hamiltonian matrix). The Lanczos algorithm for determining the eigenvalues $\{p_k(E)\}$ is thus very efficient, the number of iterations required being only the rank of the matrix, i.e., the number of non-zero eigenvalues. For the $H_2 + OH \rightarrow H_2O + H$ reaction, for example, the size of the Hamiltonian matrix is the order of $10^5 \times 10^5$, but there are only ~10 to 20 non-zero eigen reaction probabilities $\{p_k\}$, so only ~10 to 20 Lanczos iterations with $\hat{P}$ are required to obtain them.

Every Lanczos iteration with $\hat{P}$, however, requires two operatons of the Green's function onto a vector,

$$\mathbf{G}(E)(or\mathbf{G}(E)^*) \cdot \mathbf{v} \equiv \mathbf{x}, \tag{2.9a}$$

meaning that one must solve the linear system

$$(E \pm i\epsilon - \mathbf{H}) \cdot \mathbf{x} = \mathbf{v} \tag{2.9b}$$

each time, and this is the major computational task. The most powerful way discovered so far for doing this is the quasi-minimum residual (QMR) algorithm,[9,10] an iterative method that has proved to be extremely efficient (when used with preconditioning) and very economical of computer memory, requiring only a few vectors - and no matrices - to be stored.

By way of example, Fig. 2 shows the eigenreaction probabilities for the collinear $H + H_2 \rightarrow H_2 + H$ as a function of energy. One clealy sees the qualitative correspondence of these eigenvalues with the transmission probabilities of transition state theory (TST),

$$N_{TST}(E) = \sum_{n^\ddagger} P_{1d}(E - \epsilon_n{}^\ddagger), \tag{2.10}$$

where P_{1d} (E_1) is a one dimensional transmission probability as a function of the energy $E_1 = E - \epsilon_n{}^\ddagger$ available in the reaction coordinate. ($\epsilon_n{}^\ddagger$ is the vibrational enegy level for motion orthogonal to the reaction coordinate, i.e., for states of the "activated complex".) In TST each transmission probability rises from zero at the various thresholds of the activated complex energy levels and remains at unity. The eigen reaction probabilities are seen to behave qualitatively like this, but do not follow this behavior in detail because of transition state theory - violating dynamics, i.e., trajectories (in a classical picture) that re-cross the dividing surface due to the short-lived collision complex of the $H + H_2$ system.

Figure 3 shows the cumulative reaction probability N(E) for the collinear and three-dimensional versions of the $H + H_2$ reaction. The non-monotonic energy dependence seen in N(E) for the collinear case (Fig. 3a) is a result of transition state-violating dynamics. In the 3d case (Fig. 3b), however, N(E) is monotonically increasing; i.e., the additional averagings involved in 3d causes TST to be a better approximation (a well-known phenomenon).

Finally, Fig. 4 shows N(E) for the $H_2 + OH \rightarrow H_2O + H$ reaction,[11] and here one sees not only monotonic energy dependence but also the disappearance in the step structure seen in Fig. 3. This is because of the higher density of states (because of the additional degrees of freedom), causing the "steps" to overlap and thus not be apparant to the eye.

III. SEMICLASSICAL APPROXIMATION FOR THE CRP

Even with these advances described in Section II, however, rigorous quantum calculations are still feasible only for relatively simple chemical reactions. The largest molecular system studied to date using these approaches is $H_2 + OH \rightarrow H_2O + H$ for total angular momentum $J = 0$, a six degree-of-freedom system.[11] The fundamental limitation in these rigorous quantum approaches is that the number of basis functions (or grid points in a discrete variable representation[12]) grows exponentially with the number of degrees of freedom for the system, and the linear algebra calculation necessary to obtain the Green's function grows in difficulty more than linearly with the number of basis functions.

One is thus clearly interested in approximate approaches that have the potential for treating far more complex systems, but which are also of useful reliability. To this end, we have pursued a semiclassical, classical trajectory-based approach for evaluating the CRP. The semiclassical approximation for the CRP is in principle quite straight-forward: one uses Eq. (2.5) with a semiclassical approximation for the Green's function. (A similar kind of semiclassical approximation for the Green's function has also been used to obtain the S-matrix itself.[13]) For a generic cartesian Hamiltonian with f degrees of freedom, the primitive, or Van Vleck[14,15] approximation for the Green's function is

$$< \mathbf{x}_2|\hat{G}(E)|\mathbf{x}_1 > = \frac{1}{i\hbar}\int_0^\infty dt\; e^{iEt/\hbar} \sum_{\mathbf{p}_1} \left[(2\pi i\hbar)^f \left|\frac{\partial \mathbf{x}_t}{\partial \mathbf{p}_1}\right|\right]^{-1/2}$$
$$\exp\{\frac{i}{\hbar}[S(\mathbf{x}_1, \mathbf{p}_1, t) + i\epsilon_t]\} \exp(-i\pi\nu/2), \tag{3.1}$$

where $\mathbf{x}_t \equiv \mathbf{x}(\mathbf{x}_1, \mathbf{p}_1; t)$ is the classical trajectory with the indicated initial conditions, S is the classical action along the trajectory, ν (the Maslov index) is the number of zeros experienced by the Jacobian determinant along the trajectory, and ϵ_t is the exponential damping factor arising from the absorbing potential,

$$\epsilon_t \equiv \int_0^t dt'\; \epsilon(\mathbf{x}(\mathbf{x}_1, \mathbf{p}_1; t')). \tag{3.2}$$

The sum in Eq. (3.1) is over all values of the initial momentum $\mathbf{p}_1$ that satisfy the boundary condition

$$\mathbf{x}(\mathbf{x}_1, \mathbf{p}_1; t) = \mathbf{x}_2. \tag{3.3}$$

The absorbing potential factor $e^{-\epsilon_t/\hbar}$ is the only non-standard feature in Eq. (3.1). Fortunately, it is much simpler to deal with the absorbing potential *semiclassically* than it is quantum mechanically: it cannot cause any unwanted reflections in the above semiclassical expression because we have implicitly made an infinitesimal approximation for it. Thus, it does not affect the dynamics and only causes absorption; see also the disscusion by Seideman *et al.*[3b]

The key feature to making a semiclassical approach practical is to avoid having to deal explicity with the double ended boundary conditions in Eq. (3.3).[16–20] (The initial condition, $\mathbf{x}(\mathbf{x}_1, \mathbf{p}_1; 0) = \mathbf{x}_1$ is obviously easy to deal with.) To do this one uses the standard coordinate space representation of Eq. (2.5),

$$N(E) = 4 \int d\mathbf{x}_1 \int d\mathbf{x}_2 \; \epsilon_r(\mathbf{x}_1) \; \epsilon_p(\mathbf{x}_2) \; |< \mathbf{x}_2|\hat{G}(E)|\mathbf{x}_1 > |^2, \tag{3.4}$$

and the following initial value representation (IVR) for the Green's function:[19b]

$$\begin{aligned} < \mathbf{x}_2|\hat{G}(E)|\mathbf{x}_1 >^{\text{IVR}} &= \frac{1}{i\hbar(2\pi\hbar)^f} \int d\mathbf{p}_1 \int_0^\infty dt \sqrt{\frac{\partial \mathbf{p}_t}{\partial \mathbf{p}_1}} \\ &\quad \exp\{\frac{i}{\hbar}[Et + S(\mathbf{x}_1, \mathbf{p}_1, t) - \mathbf{p}_t(\mathbf{x}_t - \mathbf{x}_2) + i\epsilon_t]\}; \end{aligned} \tag{3.5}$$

this comes about by making the primitive semiclassical approximation in a momentum representation and then Fourier transorming this to obtain $< \mathbf{x}_2|G(E)|\mathbf{x}_1 >$. We found, however, that the direct use of Eq. (3.5) gives quite unstable and erratic results (*vide infra*). Excellent results are obtained, though, if Eq. (3.5) is subjected to a modified Filinov transformation (MFT) of they type used by Makri and Miller;[21] this replaces Eq. (3.5) by

$$\begin{aligned} < \mathbf{x}_2|\hat{G}(E)|\mathbf{x}_1 >^{\text{MFT}} &= \frac{1}{i\hbar(2\pi\hbar)^f} \int d\mathbf{p}_1 \int_0^\infty dt \sqrt{\frac{\partial \mathbf{p}_t}{\partial \mathbf{p}_1} - i\hbar A \frac{\partial \mathbf{x}_t}{\partial \mathbf{p}_1}} \exp[-\frac{A}{2}(\mathbf{x}_2 - \mathbf{x}_t)^2] \\ &\quad \exp\{\frac{i}{\hbar}[Et + S(\mathbf{x}_1, \mathbf{p}_1, t) - \mathbf{p}_t(\mathbf{x}_t - \mathbf{x}_2) + i\epsilon_t]\}. \end{aligned} \tag{3.6}$$

In the limit $A \to 0$, the IVR of Eq. (3.5) is regained, and as $A \to \infty$ one sees that

$$e^{-\frac{A}{2}(\mathbf{x}_2 - \mathbf{x}_t)^2} \to (\frac{A}{2\pi})^{f/2} \delta_f(\mathbf{x}_2 - \mathbf{x}_t), \tag{3.7}$$

and it is not hard to show that Eq. (3.6) then reverts to the original primitive semiclassical result for G, Eq. (3.1) (with the boundary condition, Eq. (3.3)). Eq. (3.6) is also closely related to the "cellular dynamics" approach of Heller and co-workers[18] and to some of the IVRs used by Herman *et al.*[17] and by Kay.[20]

The final expression used to generate the results discussed in the the next section is thus

$$N(E) = \frac{4}{(2\pi\hbar)^{2f}\hbar^2} \int d\mathbf{x}_1 \int d\mathbf{x}_2\, \epsilon_r(\mathbf{x}_1)\, \epsilon_p(\mathbf{x}_2) \left| \int d\mathbf{p}_1 \int_0^\infty dt \sqrt{\left|\frac{\partial \mathbf{p}_t}{\partial \mathbf{p}_1} - i\hbar A \frac{\partial \mathbf{x}_t}{\partial \mathbf{p}_1}\right|} \right.$$
$$\left. \exp\{\frac{i}{\hbar}[Et + S(\mathbf{x}_1, \mathbf{p}_1, t) - \mathbf{p}_t(\mathbf{x}_t - \mathbf{x}_2) + i\epsilon_t]\} \exp[-\frac{A}{2}(\mathbf{x}_2 - \mathbf{x}_t)^2] \right|^2 . \qquad (3.8)$$

Regarding practical aspects of the calculation, we note that for given values of the initial conditions $(\mathbf{x}_1, \mathbf{p}_1)$, the time integral in Eq. (3.8) is evaluated along the trajectory while one is computing it; *i.e.*, one does not need to store all the time dependent quantities and then do the integral over t. Doing the t-integral thus entails essentially no extra effort in the calculation. (One continues the integral over t until the absorption factor $e^{-\epsilon_t/\hbar}$ damps the integrand effectively to zero.) Also due to the structure of Eq. (3.8), one can do the calculation for many different values of the integration variable $\mathbf{x}_2$ — and also for many different values of energy E — all from the same set of initial conditions $(\mathbf{x}_1, \mathbf{p}_1)$, *i.e.*, from the same set of trajectories. The most crucial numerical aspect of the calculation is the integral of initial momenta $\mathbf{p}_1$, because the integrand has positive and negative contributions (while the integrals over $\mathbf{x}_1$ and $\mathbf{x}_2$ involve positive definite quantities). The Filinov damping factor, $\exp[-\frac{A}{2}(\mathbf{x}_2 - \mathbf{x}_t)^2]$, greatly improves this aspect of the calculation and is the principal reason why the modified Filinov representation of the Green's function is preferable to the IVR of Eq. (3.5).

Finally, note that in Eq. (2.12) we have included no Maslov phase factor related to the square root of the Jacobian determinant D,

$$D(\mathbf{x}_1, \mathbf{p}_1; t) \equiv \left|\frac{\partial \mathbf{p}_t}{\partial \mathbf{p}_1} - i\hbar A \frac{\partial \mathbf{x}_t}{\partial \mathbf{p}_1}\right|. \qquad (3.9)$$

This is because in this "hybrid representation" $D(t)$ will in general never vanish for any value of t (because $\frac{\partial \mathbf{p}_t}{\partial \mathbf{p}_1}$ and $\frac{\partial \mathbf{x}_t}{\partial \mathbf{p}_1}$ are each real). It is easy to see that the initial value $(t \to 0)$

of $D(t)$ is unity (since $\mathbf{x}_t \sim \mathbf{x}_1 + \mathbf{p}_1 t/m, \mathbf{p}_t \simeq \mathbf{p}_1$), and to obtain the correct phase of $D(t)^{1/2}$ for all later t one simply follows the complex value of $D(t)$ along the trajectory, adding the necessary phase $e^{\pm i\pi}$ anytime the branch line, $D(t) =$ a negative real number, is crossed so that $D(t)^{1/2}$ is a continuous function of t.

As a first test[22] of the semiclassical approach described above we have computed the transmission probability through the Eckart potential barrier,

$$V(x) = V_0 \operatorname{sech}^2(x), \tag{3.10}$$

with a barrier $V_0 = 0.425$ eV and the mass m = 1060 a.u. chosen, as before,[3a] to correspond approximately to the $H + H_2 \rightarrow H_2 + H$ reaction. The first important feature to show is the extent to which the Filinov "smoothing" transformation simplifies the integral over p_1. For the values $x_1 = -4.75$ a.u. and $x_2 = 4.25$ a.u., Fig. 5 shows the real part of the integral of Eq. (3.6) for several values of the parameter A ($= 0, 1.0$, and 10.0) and two values of the energy E, one below the barrier ($E = 0.3$ eV) and one above the barrier ($E = 0.6$ eV). One clearly sees the effect of the Filinov smoothing ($A > 0$) on damping the oscillatory nature of the integral. One also sees the stationary phase region of the integral for the case above the barrier, $E = 0.6$ eV, near the value of $p_1 \approx 1.0$. There is no stationary phase region for the energy below the barrier, $E = 0.3$ eV, and this is of course why the transmission probability is small in this case (*i.e.*, in the tunneling regime).

Figure 6 shows the results obtained for N(E) for several values of A. We do not obtain satisfactory results for A = 0, but for a wide range of $A > 0$ we obtain quite stable results that are relatively insensitive to the particular value of this smoothing parameter. This is precisely the behavior one wishes to see. It is also significant that the results in Fig. 6 are accurate for some ways into the "classically forbidden" tunnelling regime, in this case for energies as much as 0.1 eV or so below the barrier, down to a transmission probability of $\approx 10^{-3}$.

IV. CONCLUDING REMARKS

One thus has a theoretical methodology that allows one to compute the rate constant for a chemical reaction "directly", without having to solve the complete state-to-state reactive scattering problem, yet also "correctly", without inherent approximation. One can of course carry out the "correct" quantum calculation only for relatively small molecular systems, but it is possible to utilize a semiclassical approximation (which includes the effects of interference and tunneling) that should be applicable to larger systems.

ACKNOWLEDGMENTS

This work was supported by the Director, Office of Energy Research, Office of Basic Energy Sciences, Chemical Sciences Division of the U. S. Department of Energy under Contract No. DE-AC03-76SF00098.

REFERENCES

1. W. H. Miller, J. Chem. Phys. **62**, 1899 (1975).

2. W. H. Miller, S. D. Schwartz, and J. W. Tromp, J. Chem. Phys. **79**, 4889 (1983).

3. (a) T. Seideman and W. H. Miller, J. Chem. Phys. **96**, 4412 (1992);
   (b) T. Seideman and W. H. Miller, J. Chem. Phys. **97**, 2499 (1992).

4. U. Manthe and W. H. Miller, J. Chem. Phys. **99**, 3411 (1993).

5. (a) An interesting set of papers by many of the founders of the theory - Wigner, M. Polanyi, Evans, Eyring – is in Trans. Faraday Soc. **34**, Reaction Kinetics - A General Discussion, 1938, pp. 1-127.
   (b) P. Pechukas, in Dynamics of Molecular Collisions, Part B, ed. W. H. Miller (Vol. 2 of Modern Theoretical Chemistry), Plenum, NY, 1976, Chapter 6.
   (c) D. G. Truhlar, W. L. Hase, and J. T. Hynes, J. Chem. Phys. **87**, 2664 (1983).

6. W. H. Miller, Accts. Chem. Res. **26**, 174 (1993).

7. D. Thirumalai, B. C. Garrett, and B. J. Berne, J. Chem. Phys. **83**, 2972 (1985).

8. See also
   (a) A. Goldberg and B. W. Shore, J. Phys. B **11**, 3339 (1978);
   (b) C. Leforestier and R. E. Wyatt, J. Chem. Phys. **78**, 2334 (1983);
   (c) C. Cerjan, D. Kosloff, and T. Teshef, Geophysics **50**, 705 (1985);
   (d) R. Kosloff and D. Kosloff, J. Comput. Phys. **63**, 363 (1986);
   (e) D. Neuhauser and M. Baer, J. Chem. Phys. **90**, 4351 (1989);
   (f) D. Neuhauser, M. Baer, and D. J. Kouri, J. Chem. Phys. **93**, 2499 (1990);
   (g) D. Neuhauser, J. Chem. Phys. **93**, 7836 (1990).

9. R. W. Freund, SIAM J. Sci. Stat. Comput. **13**, 425 (1992).

10. H. O. Karlsson, J. Chem. Phys. **101**, 0000 (1995).

11. (a) U. Manthe, T. Seideman, and W. H. Miller, J. Chem. Phys. **99**, 10078 (1993);
    (b) U. Manthe, T. Seideman, and W. H. Miller, J. Chem. Phys. **101**, 4759 (1994).

12. J. C. Light, I. P. Hamilton, and J. V. Lill, J. Chem. Phys. **82**, 1400 (1985).

13. S. Keshavamurthy and W. H. Miller, Chem. Phys. Lett. **218**, (1994) 189.

14. J. H. Van Vleck, Proc. Natl. Acad. Sci. **14**, 178 (1928).

15. See also reviews and applications in

(a) W. H. Miller, Adv. Chem. Phys. **25**, 69 (1974); **30**, 77 (1975);

(b) V. P. Maslov and M. V. Fedoriuk, *Semiclassical Approach in Quantum Mechanics*, Reidel Pub. Co., Boston, 1981;

(c) M. C. Gutzwiller, *Chaos in Classical and Quantum Mechanics*, Springer, NY, 1990.

16. (a) W. H. Miller, J. Chem. Phys. **53**, 3578 (1970);

(b) W. H. Miller and T. F. George, J. Chem. Phys. **56**, 5668 (1972);

(c) See ref. 16a;

(d) W. H. Miller, J. Chem. Phys. **95**, 9428 (1991).

17. (a) M. F. Herman and E. Kluk, Chem. Phys. **91**, 27 (1984);

(b) E. Kluk, M. F. Herman, and H. L. Davis, J. Chem. Phys. **84**, 326 (1986);

(c) M. F. Herman, J. Chem. Phys. **85**, 2069 (1986).

18. (a) E. J. Heller, J. Chem. Phys. **94**, 2723 (1991);

(b) M. A. Sepulveda and E. J. Heller, J. Chem. Phys. **101**, 8004 (1994);

(c) E. J. Heller, J. Chem. Phys. **95**, 9431 (1991).

19. (a) G. Campolieti and P. Brumer, J. Chem. Phys. **96**, 5969 (1992);

(b) G. Campolieti and P. Brumer, Phys. Rev. A **50**, 997 (1994).

20. (a) K. G. Kay, J. Chem. Phys. **100**, 4377 (1994);

(b) K. G. Kay, J. Chem. Phys. **100**, 4432 (1994);

(c) K. G. Kay, J. Chem. Phys. **101**, 2250 (1994).

21. (a) N. Makri and W. H. Miller, Chem. Phys. Lett. **139**, 10 (1987);

(b) N. Makri and W. H. Miller, J. Chem. Phys. **89**, 2170 (1988).

22. B. W. Spath and W. H. Miller, J. Chem. Phys. **XX**, 0000 (1995).

FIGURES

FIG. 1. Solid lines are contours of the potential energy surface for the $H + H_2 \rightarrow H_2 + H$ reaction. Broken lines are contours of the absorbing potential (which is zero in the central part of the interaction region and turned on at the edge), for three possible choices of it. The points are the grid points which constitute the basis set for the evaluation of the quantum trace, Eq. (2.5).

FIG. 2. The dotted lines are the eigen reaction probabilities $\{p_k(E)\}$ for the collinear $H + H_2$ reaction. The solid line is their sum, the cumulative reaction probability N(E).

FIG. 3. Cumulative reaction probability for the $H + H_2 \rightarrow H_2 + H$ reaction, (a) for collinear geometry (ref. 3a), (b) three dimensional space for total angular momentum J=0 (ref. 3b).

FIG. 4. The cumulative reaction probability for the $H_2 + OH \rightarrow H_2O + H$ reaction as a function of total energy, for total angular momentum J=0 (ref. 11); (a) logarithmic scale, (b) linear scale.

FIG. 5. The real part of integrand of Eq. (3.6) as a function of p_1, for $x_1 = -4.75$ a.u. and $x_2 = 4.25$ a.u., for the two indicated values of total energy and three different values of the Filinov parameter A = 0.0, 1.0, and 10.0 (top, middle, and bottom, respectively).

FIG. 6. N(E) vs energy E for several values of the Filinov parameter, (□) A = 0.0, (○) A = 1.0, (◇) A = 5.0, (●) A = 20.0, compared to the exact quantum result (–).

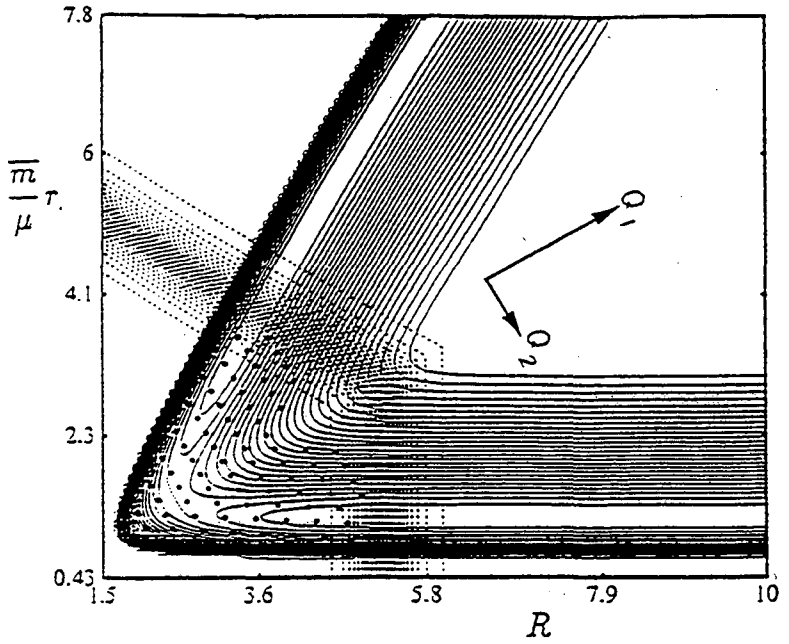
7.8
6
4.1
2.3
0.43
1.5
3.6
5.8
7.9
10
R
$\sqrt{\frac{m}{\mu}}\tau$
Q_1
Q_2

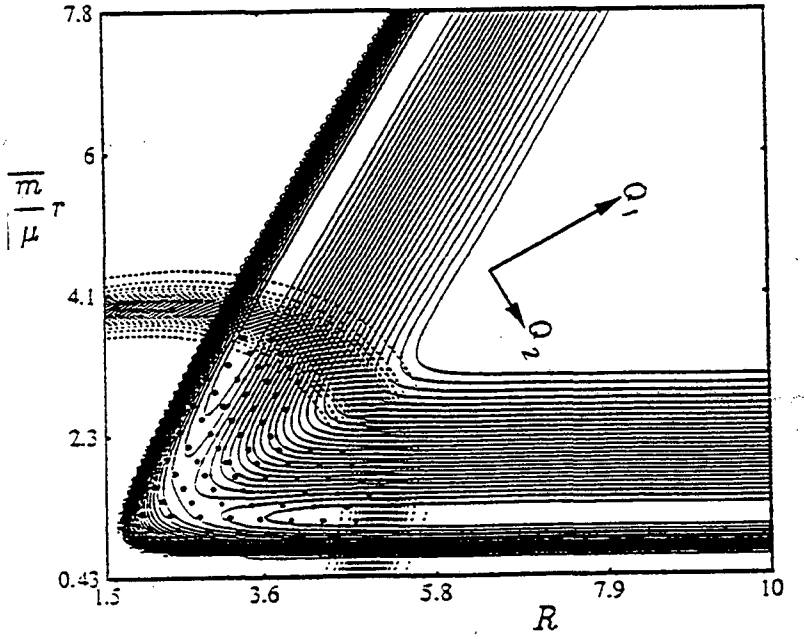
7.8
6
4.1
2.3
0.43
1.5
3.6
5.8
7.9
10
R
$\sqrt{\frac{m}{\mu}}\tau$
Q_1
Q_2

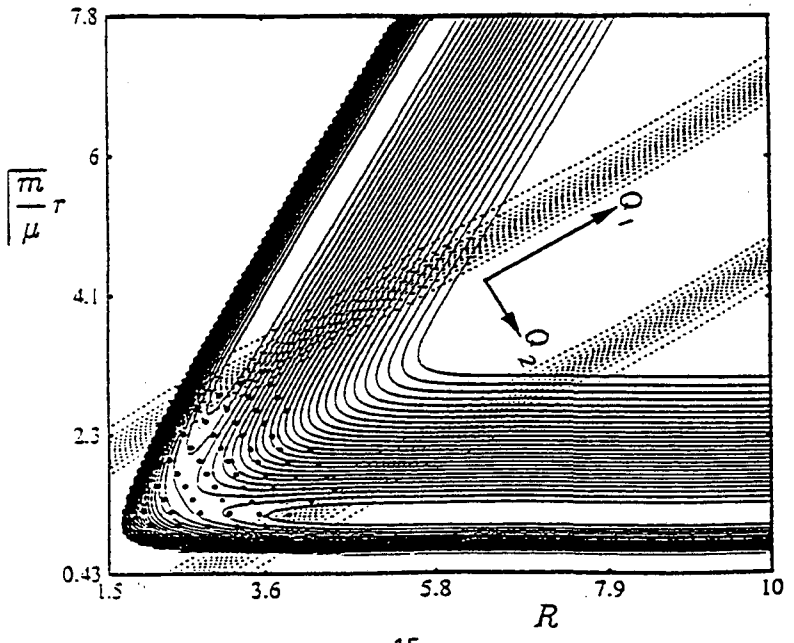
7.8
6
4.1
2.3
0.43
1.5
3.6
5.8
7.9
10
R
$\sqrt{\frac{m}{\mu}}\tau$
Q_1
Q_2

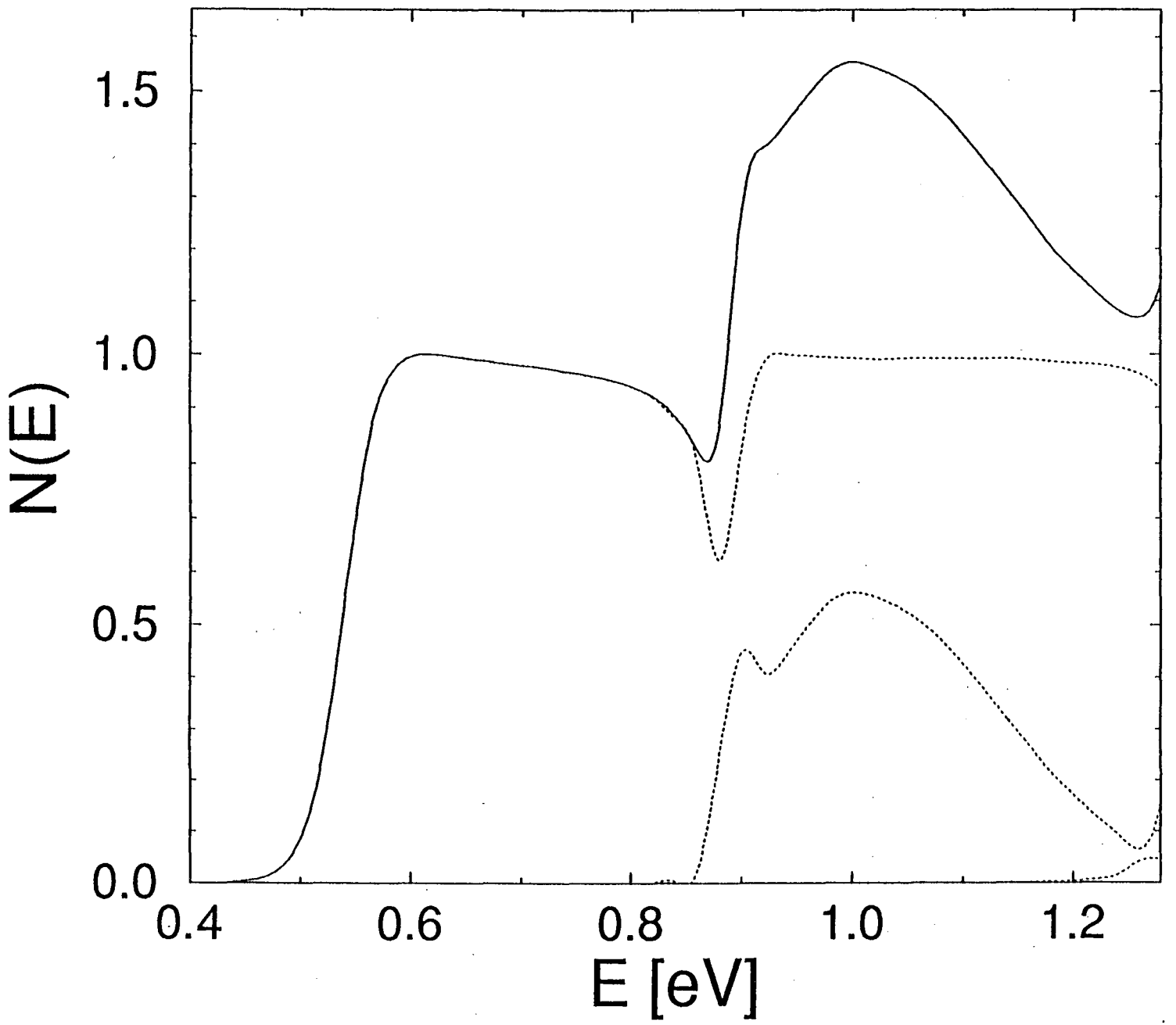
1.5
1.0
0.5
0.0
N(E)
0.4
0.6
0.8
1.0
1.2
E [eV]

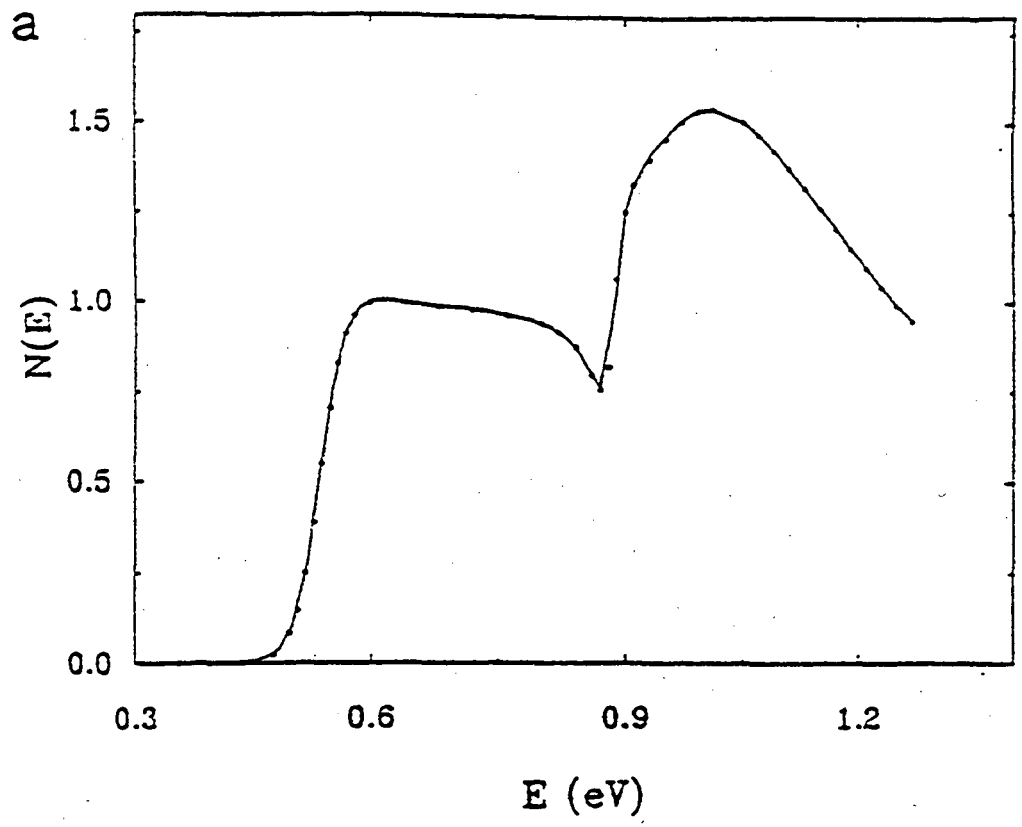
a
1.5
1.0
0.5
0.0
N(E)
0.3
0.6
0.9
1.2
E (eV)

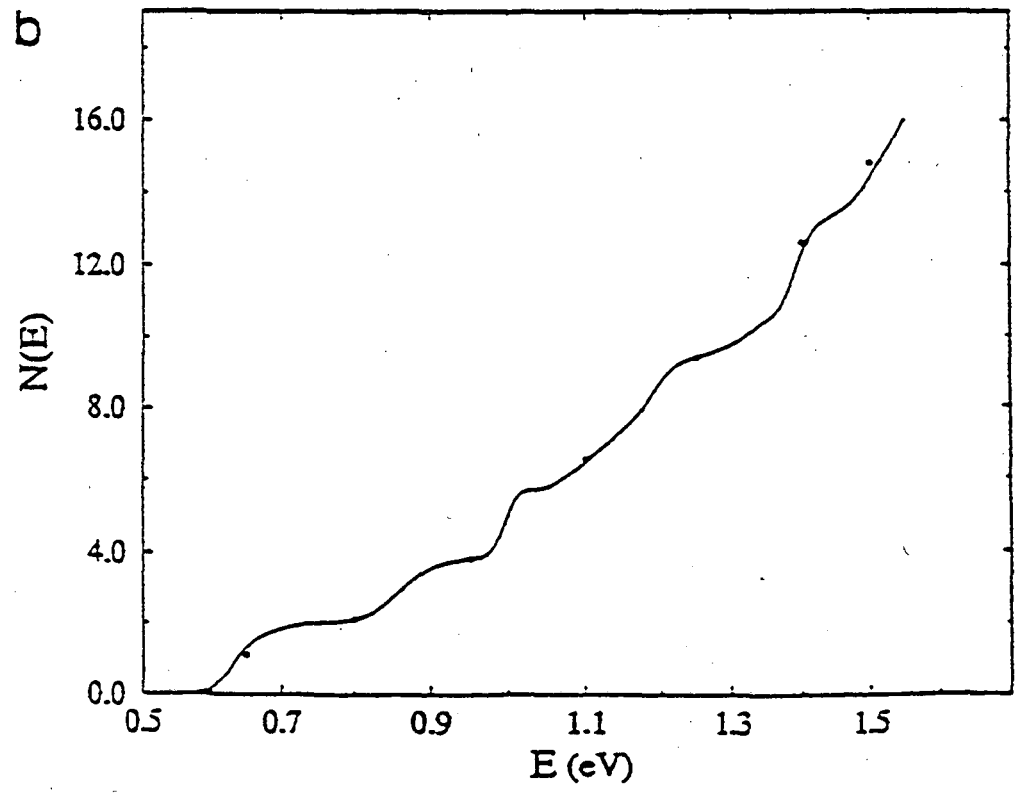
b
16.0
12.0
8.0
4.0
0.0
N(E)
0.5
0.7
0.9
1.1
1.3
1.5
E (eV)

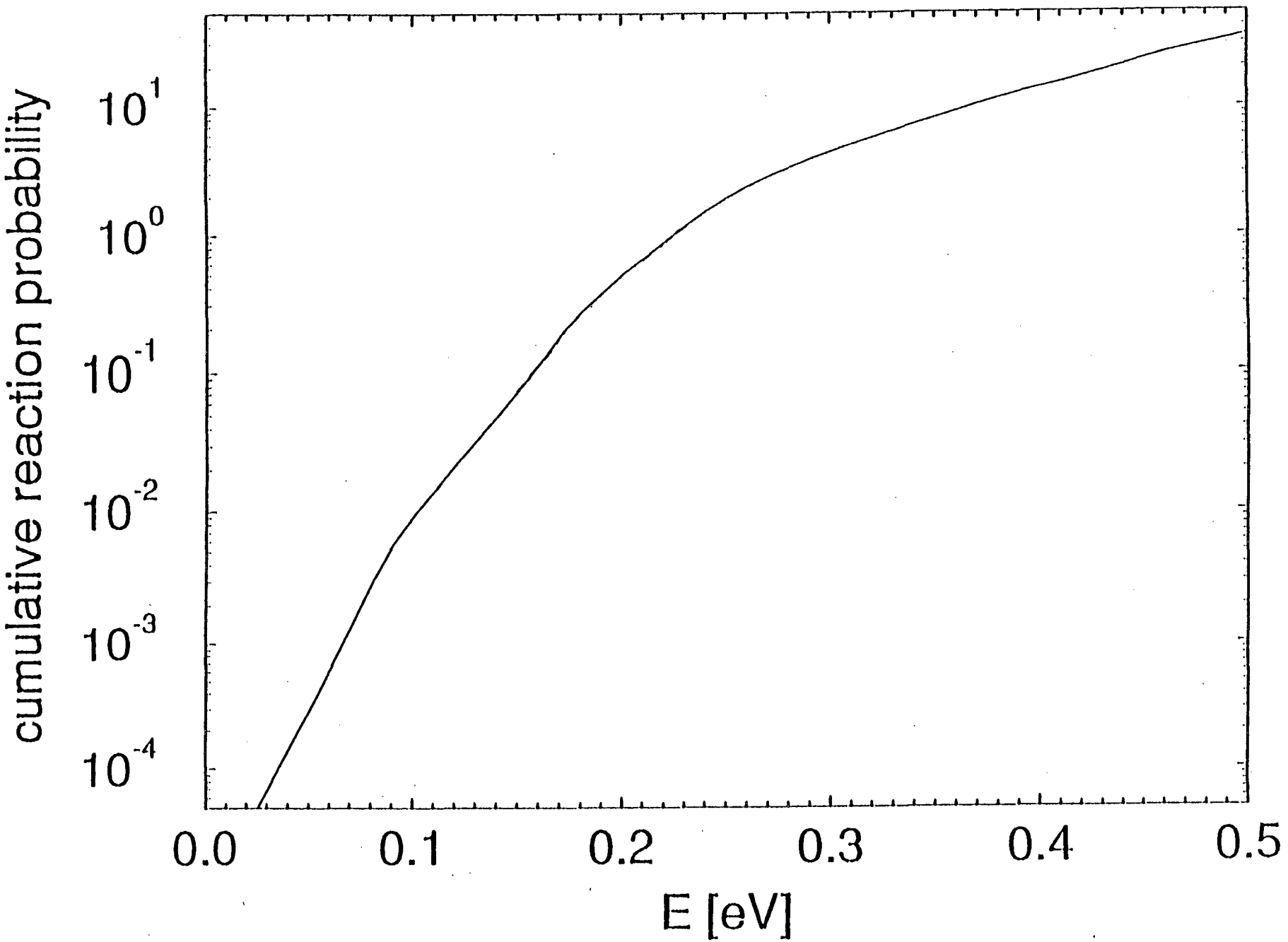
cumulative reaction probability
10^{1}
10^{0}
10^{-1}
10^{-2}
10^{-3}
10^{-4}
0.0
0.1
0.2
0.3
0.4
0.5
E [eV]

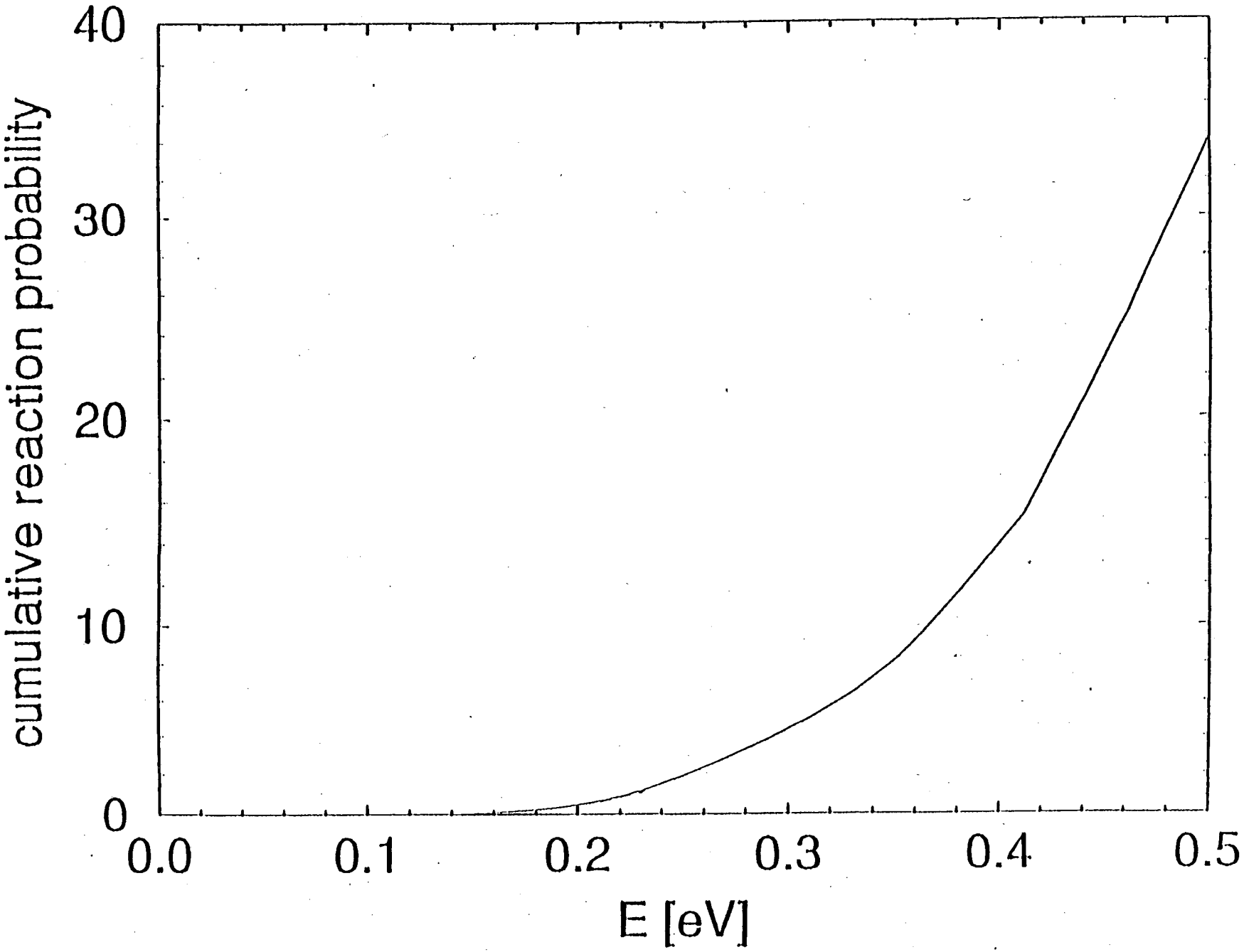
cumulative reaction probability
40
30
20
10
0
0.0
0.1
0.2
0.3
0.4
0.5
E [eV]

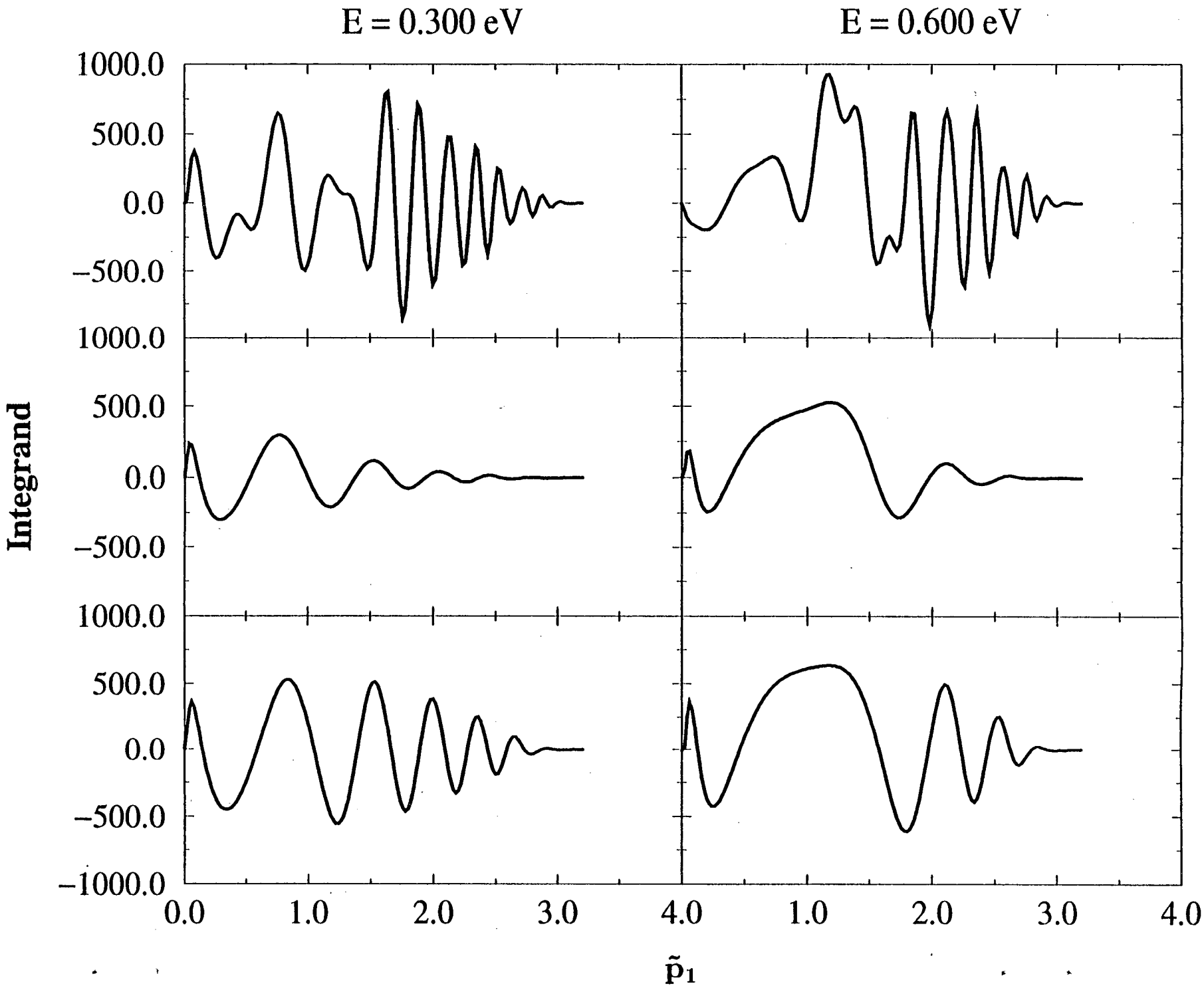
E = 0.300 eV
E = 0.600 eV
Integrand
1000.0
500.0
0.0
−500.0
−1000.0
0.0
1.0
2.0
3.0
4.0
$\tilde{p}_1$

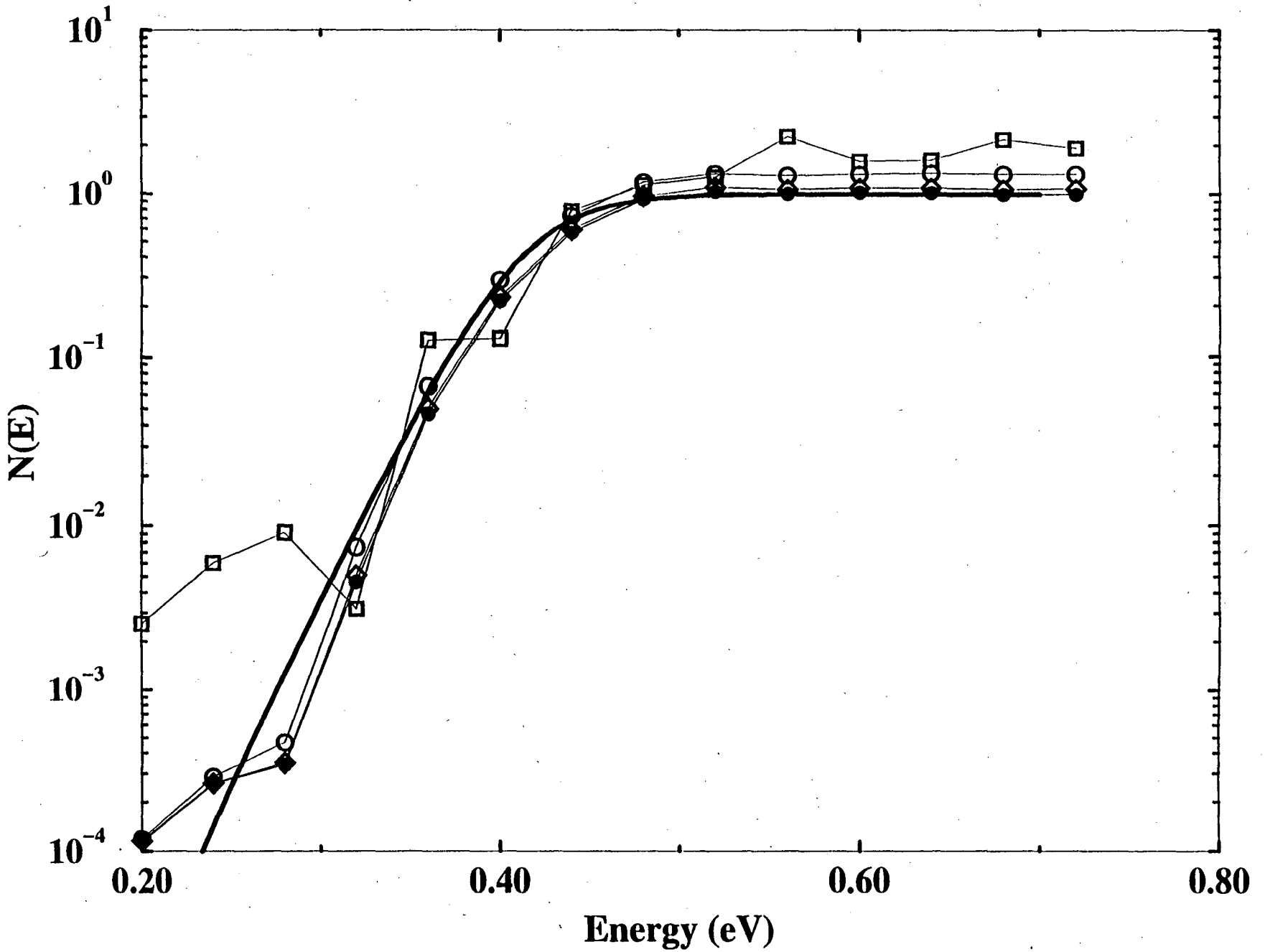
10^1
10^0
10^{-1}
10^{-2}
10^{-3}
10^{-4}
N(E)
0.20
0.40
0.60
0.80
Energy (eV)

LAWRENCE BERKELEY NATIONAL LABORATORY
UNIVERSITY OF CALIFORNIA
TECHNICAL & ELECTRONIC INFORMATION DEPARTMENT
BERKELEY, CALIFORNIA 94720